PLGA-based particulate vaccine delivery systems for immunotherapy of cancer

Monteiro Garrido Castro e Silva, Ana Luisa

Chapter 3

Poly-(lactic-co-glycolic-acid)-based particulate vaccines: particle uptake by dendritic cells is a key parameter for immune activation

Ana Luisa Silva*, Rodney A. Rosalia*, Eleni M. Varypataki, Shanti Sibuea, Ferry Ossendorp, Wim Jiskoot

*contributed equally to this study

Vaccine 2015 33(7):847-54

Abstract

Poly(lactic-co-glycolic acid) (PLGA) particles have been extensively studied as biodegradable delivery system to improve the potency and safety of protein-based vaccines. In this study we analyzed how the size of PLGA particles, and hence their ability to be engulfed by dendritic cells (DC), affects the type and magnitude of the immune response in comparison to sustained release from a local depot. PLGA microparticles (MP, volume mean diameter ≈ 112 µm) and nanoparticles (NP, Z-average diameter ≈ 350 nm) co-encapsulating ovalbumin (OVA) and poly(I:C), with comparable antigen (Ag) release characteristics, were prepared and characterized. The immunogenicity of these two distinct particulate vaccines was evaluated *in vitro* and *in vivo*. NP were efficiently taken up by DC and greatly facilitated MHC I Ag presentation *in vitro*, whereas DC cultured in the presence of MP failed to internalize significant amounts of Ag and hardly showed MHC I Ag presentation. Vaccination of mice with NP resulted in significantly better priming of Ag-specific $CD8^+$ T cells compared to MP and OVA emulsified with incomplete Freund's adjuvant (IFA). Moreover, NP induced a balanced TH1/TH2-type antibody response, compared to vaccinations with IFA which stimulated a predominant TH2-type response, whereas MP failed to increase antibody titers. In conclusion, we postulate that particle internalization is of crucial importance and therefore particulate vaccines should be formulated in the nano- but not micro-size range to achieve efficient uptake, significant MHC class I cross-presentation and effective T and B cell responses.

Keywords: Protein antigen, PLGA, microparticles, nanoparticles, adjuvants, immunotherapy, cellular immune response

1. Introduction

In the past few years, extensive efforts in the immunotherapy field have led to the development of several therapeutic vaccine strategies [1-3]. Protein vaccines are popular forms of therapeutic vaccines [3, 4] which have been tested successfully in (pre-) clinical studies against various immunological diseases [5, 6]. The potency of protein vaccines can be significantly amplified via the encapsulation in biodegradable particles. The use of particles facilitates the uptake of the antigen (Ag) by dendritic cells (DC), allows the co-delivery of Ag and Toll-like receptor ligands (TLRL) [7, 8] and improves Ag processing, presentation and T cell priming by DC compared to use of soluble Ag. Generally, particulate Ag is better routed into MHC class I cross-presentation pathways and preserved inside intracellular compartments, resulting in sustained and efficient priming of $CD8^+$ T cell responses [9-13]. DC have superior capacity to cross-present exogenous Ag in MHC I molecules and are considered the major target for vaccines aimed at activating a robust $CD8^+$ T cell mediated immunity [3, 14]

Most clinical trials for cancer immunotherapy have relied on the use of Montanide, a GMP-grade version of incomplete Freund's adjuvant (IFA), which is a water-in-oil (w/o) emulsion for Ag delivery. The immune-activating properties of Montanide are partially

explained through the formation of a local Ag depot and the onset of inflammation, which attracts immune cells towards the site of injection [15] where the Ag is taken up primarily in its soluble form [16]. However, the use of Montanide is associated with significant local adverse effects [5], reason why there is an urgent need for alternatives [17].

Nanoparticles (NP) and microparticles (MP) prepared from biodegradable poly(L-lactic-co-glycolic acid) (PLGA) have been studied extensively for the sustained delivery of proteins and therapeutic agents and as an potential alternative to w/o emulsions [18-20]. Plain PLGA particles have sub-optimal adjuvant properties *in vivo* resulting in poor DC maturation [9, 21], which can be overcome by the inclusion of TLRL, leading to an efficient induction of TH1-mediated T cell responses with the capacity to control tumors or protect against a viral challenge [7, 22-25].

It is generally assumed that NP, compared to MP, are better for targeted drug delivery due to a better biodistribution [26, 27] and ability to cross biological barriers [28]. Still, there is little agreement when it comes to therapeutic vaccines: which size leads to the most efficient MHC class I Ag cross-presentation remains controversial [29-31].

To study the importance of particle uptake for the induction of an immune response, we developed NP and MP containing equivalent amounts of Ag and TLRL with comparable release profiles *in vitro*. Particles co-encapsulating model Ag ovalbumin (OVA) and TLR3L poly(I:C) were formulated to obtain NP that will be efficiently internalized by DC [32], releasing the Ag mostly intracellularly [12], versus MP with a size (> 20 μm) that is too large to be taken up by DC [31], thus functioning exclusively as a local Ag/TLR3L depot under the skin, similarly to Montanide.

2. Materials and Methods

2.1. Reagents

PLGA Resomer RG502H (50:50 MW 5,000–15,000 Da) was purchased from Boehringer Ingelheim (Ingelheim am Rhein, Germany); PLGA Resomer RG752H (75:25 MW 4,000-15,000 Da), Dichloromethane (DCM), dimethyl sulfoxide (DMSO), and Hepes from Sigma–Aldrich (Steinheim, Germany); Ovalbumin (OVA) grade V, 44 kDa from Worthington (New Jersey, USA); Alexa Fluor 488 (AF488) labeled OVA from Invitrogen (Merelbeke, Belgium); Tween 20 from Merck Schuchardt (Hohenbrunn, Germany); polyvinyl alcohol (PVA) 4 – 88 (31 kDa) from Fluka (Steinheim, Germany); Poly(I:C) LMW and rhodamine labeled poly(I:C) from InvivoGen (San Diego, USA); Phosphate-buffered saline (NaCl 8.2 g/L; Na2HPO4.12 H2O 3.1 g/L; NaH2PO4.2H2O 0.3 g/L) (PBS) from B. Braun (Melsungen, Germany); all fluorescently labeled antibodies from BD Pharmingen (San Diego, USA); incomplete Freund's adjuvant (IFA) from Difco Laboratories (Detroit, USA). APC-SIINFEKL/H2-Kb tetramers, SIINFEKL (OVA8) and ASNENMETM (FLU9)

and carboxyfluorescein succinimidyl ester (CFSE)-labeled synthetic short peptides were produced in house. All other chemicals were of analytical grade and aqueous solutions prepared with Milli-Q water.

2.2. Cells

D1 cells, a murine GM-CSF dependent immature dendritic cell line, were cultured as described previously [33]. Bone-marrow derived DC (BMDC) were freshly isolated from femurs from mice and cultured as published previously [34] and yielded cells which were at least 90% positive for murine DC marker CD11c. B3Z $CD8^+$ T-cell hybridoma cell line, specific for the H-2Kb-restricted OVA257–264 CTL epitope SIINFEKL was cultured as described before [35].

2.3. Animals

C57BL/6 (Ly5.2/CD45.2; H-2b) mice were obtained from Charles River Laboratories. Ly5.1/CD45.1 congenic (C57BL/6 background) mice were bred in the specific pathogen-free animal facility of the Leiden University Medical Center. All animal experiments were approved by the animal experimental committee of Leiden University.

2.4. Preparation and characterization of OVA- and poly(I:C)-loaded PLGA particles

2.4.1. Preparation of NP and MP and IFA

PLGA 50:50 and PLGA 75:25 NP were prepared as described [36], using 1 mg OVA, 0.25 mg poly(I:C) and 1 µg poly(I:C)-rhodamine dissolved in 85 µl of 25 mM Hepes, pH 7.4, as inner aqueous phase. For NP and MP used in the release and uptake studies, 1% (w/w total OVA) of OVA-AF488 was added to the inner phase during preparation for detection purposes.

PLGA 50:50 MP were prepared by adding 1 mg OVA, 0.25 mg poly(I:C), and 1 µg poly(I:C)-rhodamine dissolved in 500 µl of 25 mM Hepes pH 7.4 to 1 ml DCM containing 125 mg PLGA 50:50. The mixture was homogenized for 30 s at 25,000 rpm (Heidolph Ultrax 900, Sigma, Germany) and transferred to 10 ml of 2% (w/v) PVA under magnetic stirring for 10 min at 750 rpm at room temperature, followed by 1 hour at 500 rpm at 40ºC to allow evaporation of DCM. MP were harvested and washed twice by centrifugation (2000 g, 2 min). To separate particles bigger than 20 µm, MP were diafiltrated with 3 L water under continuous stirring, using a Solvent Resistant Stirred

Cell (Milipore, USA) filtration system with a 20-µm stainless steel sieve (Advantech, USA), the retentate collected and particles recovered by centrifugation at 2000 g for 2 min. Particles >200 µm were eliminated by filtration through a 200-µm stainless steel sieve (Advantech, USA). Intactness of MP before and after filtration (see **Supplemental Figure 1**) was verified with an Axioskop microscope, equipped with Axiocam ICc 5 (Carl Zeiss, Munich, Germany) and 20x amplification objective. Images were collected with ProgRes CapturePro v2.8.8 software (Jenoptik AG, Jena, Germany). Both NP and MP suspensions were aliquoted and freeze-dried.

Preparation of IFA emulsion was performed by dissolving OVA and poly(I:C) in PBS and mixing with IFA for 30 min in a 1:1 ratio by using a vortex mixer.

2.4.2. Characterization of NP and MP

Size and polydispersity index (PDI) of NP in 5 mM Hepes pH 7.4 were determined by dynamic light scattering (DLS) using a NanoSizer ZS (Malvern Instruments, Malvern, UK). Zeta potential (ZP) was determined by laser Doppler velocimetry using the same apparatus. Size distribution of MP was determined by light obscuration (LO) using a PAMAS SVSS system (PAMAS GmbH, Rutesheim, Germany) equipped with HCB-LD-25/25 sensor and 1-ml syringe. Each sample was measured three times, each measurement consisting of three runs of 0.2 ml at a flow rate of 10 ml/min.

Encapsulation efficiency (EE) was calculated by fluorescence of OVA-AF488 (excitation 495 nm, emission 520 nm) or poly(I:C)-rhodamine (excitation 546 nm, emission 576 nm) detected in the supernatant with Infinite® M 1000 Pro (Tecan, Switzerland) microplate reader.

To study release kinetics NP/MP containing fluorescently labeled OVA and poly(I:C) were resuspended in PBS, containing 0.01% Tween 20 and 0.01% sodium azide, at 10 mg PLGA/ml, and maintained at 37ºC under tangential shaking at 100 rpm in a GFL 1086 shaking water bath (Burgwedel, Germany) for 30 days. At regular time intervals, 250 µl aliquots were taken and centrifuged for 20 min at 18000 g. Supernatants were stored at 4ºC until fluorescence intensity was determined (Infinite® M 1000 Pro, Tecan, Switzerland) [37]. OVA concentrations on remaining supernatant samples from the final day were also analyzed by BCA assay (Pierce, Rockford, IL, USA) after dissolving particles in DMSO and 0.5 M NaOH + 0.5% SDS as described [38] to validate fluorescence measurements, with comparable results (**Supplemental Table 1**).

2.5. Analysis of particle uptake by DC

Particle uptake by DC was determined by plating out D1 cells in 96-well plates (105 cells/well) and pre-cooling on ice (10 min). Pre-cooled cells were cultured for 1 h at 4ºC (on ice) or at 37ºC in the presence of PLGA particles containing OVA-AF488. After

incubation, cultured cells were washed and centrifuged twice with cold saline buffer to remove unbound particles and cells fixed with 4% paraformaldehyde (100 µl/well). Fixation was blocked by addition of 100 µl/well fetal calf serum (FCS) and washing with cold PBS. Cells were kept at room temperature and stained with rat anti-mouse CD45.2-APC fluorescent antibodies to allow detection of cells positive for particle association, based on OVA-AF488 fluorescence (excitation 495 nm, emission 520 nm) as analyzed using a BD LSRII flow cytometer. Data were acquired using the BD FACS DIVA software and analyzed with Flow Jo software (treestar).

2.6. MHC class I Ag presentation

DC were incubated for 2 h with PLGA-OVA formulations at the indicated concentrations, washed and followed by an overnight incubation (37ºC) in the presence of B3Z $CD8^+$ T cell hybridomas to measure MHC class I presentation as described previously [39]. To determine the relative maximum B3Z T cell activation, DC were loaded with the minimal epitope SIINFEKL and the extinction value set as 100% (OD590nm = 2.53 = 100%).

2.7. Vaccination studies

Animals were vaccinated with PLGA-OVA/poly(I:C) formulations, soluble OVA/poly(I:C) in PBS, or OVA/poly(I:C) emulsified in IFA by s.c. injection into the right flank on day 0 and day 28. Priming of cytotoxic $CD8^+$ T cells was assessed seven days after the 1st and 14 days after the 2nd vaccination by transferring splenocytes prepared from congenic Ly5.1 C57BL/6 animals which were pulsed with SIINFEKL (OVA8, vaccine specific target cells) or ASNENMETM (FLU9, vaccine non-specific control target cells). Target cells were labeled with either 10 µM OVA8- or 0.5 µM FLU9-CFSE. Cells were mixed 1:1 and 107 total cells were injected intravenously into the vaccinated animals. 18 h later, animals were sacrificed and single cell suspensions were prepared from isolated spleens [9]. Injected target cells were distinguished by APC-conjugated rat anti-mouse CD45.1 mAb (BD Pharmingen, San Diego, USA). *In vivo* cytotoxicity was determined by flow cytometry after 18 h using **equation 1**:

$$\%\,\text{OVA - specific killing} = \left(1 - \left[\left(\frac{OVA_8 - CFSE - peak\ area}{FLU_9 - CFSE - peak\ area}\right)^{vaccinated\ animals} \times \left(\frac{OVA_8 - CFSE - peak\ area}{FLU_9 - CFSE - peak\ area}\right)^{non-vaccinated\ animals}\right]\right) \times 100 \quad (1)$$

OVA-specific $CD8^+$ T cells present in the spleens were analyzed by co-staining with APC-conjugated SIINFEKL/H2-Kb tetramers, AF488-conjugated anti-mouse CD8α

mAb and V500-conjugated rat anti-mouse CD3 mAb. Flow cytometry was performed as described above.

2.8. Detection of antibody responses

Antibody responses were determined by collecting serum samples on day 21 (1 week before 2nd vaccination) and on day 35 (1 week after 2nd vaccination). IgG1, IgG2a and IgG2b titers against OVA were determined by ELISA. In brief, high absorbent 96-wells Nunc immunoplates were coated with 5 µg/ml OVA in PBS and incubated with titrated serum samples in 10% FCS in PBS. Antibodies were detected using streptavidine conjugated rabbit anti-murine IgG1, IgG2a and IgG2b mAb, followed by addition of horse-radish-peroxidase conjugated biotin. 3,3',5,5'-Tetramethylbenzidine (TMB) was used as a substrate and the color conversion was stopped after 10 min with 0.16 M H2SO4, which was then measured on a spectrophotometer by absorbance at 450 nm (OD450nm). To determine immune polarization the IgG2a/IgG1 ratios were determined using OD450nm values determined at 1:100 dilution if values applied were ≥ 2-fold OD450nm of the negative control (sera from non-immunized mice).

3. Results and Discussion

Particulate vaccines are promising modalities as the immune system reacts more vigorously to vaccines presented in a particulate form compared to soluble ones [9, 10]. However, the exact parameters needed to achieve robust immune responses against particulate vaccines are still a matter of debate [29-31]. This may be related to different parameters that can direct the type and potency of the immune response [40, 41], such as the route of administration upon vaccination and Ag release kinetics [27, 42, 43]. The latter is critical as sustained Ag release is essential to properly stimulate DC [44]. We have recently shown that low-burst release of encapsulated Ag is crucial for efficient MHC class I Ag presentation and $CD8^+$ T cell activation [39]. Of importance, there exists a strong correlation between (particle) size and the efficiency of Ag uptake, processing and presentation by APC [29, 32, 42].

APC may take up and process Ag with similar dimensions to pathogens, such as viruses and bacteria, with the size influencing the mechanisms of uptake and processing by APC [45]. It has been reported that particles in the range of 20-200 nm are efficiently taken up by DC and facilitate the induction of cellular immune responses, whereas particles of 0.5-5 µm mainly generate humoral responses; limited uptake of 10 µm or larger particles was observed, leading to defective immune activation [29, 31, 46]. Also, nano-sized particles supported DC maturation by TLR9 triggering in contrast to micro-sized particles [31]. These studies suggest that the efficient internalization of particles significantly dictates the ensuing vaccine induced immune response. In contrast, others have reported that vaccinations with MP also induce CTL responses, comparable to IFA- or Montanide-based delivery systems [17, 47].

Using PLGA particles co-encapsulating protein Ag and a TLR3L, we compared NP (which can be engulfed by DC) with > 20-µm MP (which are too large to be taken up) for their capacity to induce MHC class I cross-presentation *in vitro* and improve immune responses *in vivo*. To study the effect of particle uptake on the subsequent immune response, we designed NP and MP of similar compositions and with similar release properties. So, we engineered MP (PLGA 50:50) to match the release properties of NP by adding salt to the inner water phase to increase porosity and accelerate drug diffusion and release (see Supplemental **Figure 2** for inner phase compositions) [48-51]. MP were also diafiltrated to eliminate particles smaller than 20 µm that could be internalized by DC, as well as particles larger than 200 µm, and size distribution before and after filtration was determined (**Supplemental Table 2** & **Supplemental Figure 3**). Number-based mean-diameter of MP increased from 5±1 µm before filtration (BF) to 17±5 µm after filtration (AF), showing that the filtration step effectively decreased the number of particles smaller than 20 µm. Importantly, volume-based mean-diameters indicate that less than 1% of the total volume, and consequently less than 1% of the OVA content, corresponded to particles smaller than 20 µm, making it unlikely that residual particles <20 µm would have a significant effect on Ag uptake, MHC class I Ag presentation and $CD8^+$ T cell activation. Physicochemical characterization of all formulations was done in terms of encapsulation efficiency (EE), drug loading (DL), size, PDI and ZP as summarized in **Table 1** (for NP size distributions see **Supplemental Figure 4**).

Table 1: Physical characteristics of OVA/poly(I:C)-loaded PLGA NP and MP in terms of size (Z-average obtained by DLS for NP; and number (n) and volume (v) average obtained by LO for MP), PDI, ZP, EE and DL.*

Formulation	Size	PDI	ZP (mV)	OVA		Poly I:C	
				EE (%)	DL (%)	EE (%)	DL (%)
NP 50: 50	357 ± 25 nm	0.16 ± 0.03	-41 ± 7	52 ± 7	2.01 ± 0.27	66 ± 8	0.63 ± 0.07
NP 75: 25	400 ± 16 nm	0.25 ± 0.02	-25 ± 3	75 ± 1	2.87 ± 0.03	59 ± 7	0.56 ± 0.07
MP 50: 50	17 ± 5 µm (n) 112 ± 26 µm (v)	n/a	-14 ± 3	86 ± 2	0.68 ± 0.01	81 ± 2	0.16 ± 0.00

* Values represent mean +/- standard deviation of 3 independently prepared batches

PDI: polydispersity index; ZP: Zeta-potential; EE: encapsulation efficiency; DL: drug loading.

As release studies showed faster Ag and TLR3L release from NP 50:50 compared to MP 50:50, NP were also prepared with PLGA 75:25, which is more hydrophobic and therefore degrades slower, to achieve particles comparable in size to NP 50:50 and closer in release kinetics to MP 50:50. Release studies showed sustained release over 30 days (**Figure 1**) with NP 75:25 exhibiting similar long-term release characteristics to MP, but remaining closer to NP 50:50 in the early stages (<10 days), due to higher burst release. These profiles contrast with a previous study by Joshi et al. (2013) where drastic differences in release kinetics were observed: whereas the initial (burst) release

accounted for nearly total Ag and TLRL release from 300-nm NP, the release from MP with a size of about 17 μm was only 10% after 15 days [31]. Besides the difference in size, this could have contributed to the distinct immunological properties of their NP and MP formulations.

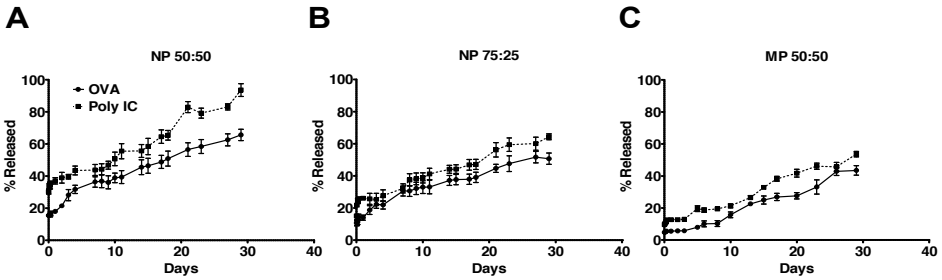

Figure 1: *In vitro* release kinetics of OVA and poly(I:C) from NP and MP. OVA (closed circles) and poly(I:C) (closed squares) release in PBS/0.01% Tween-20/0.01% NaN3 (pH 7.4) of A) NP 50:50, B) NP 75:25, and C) MP 50:50 were monitored for 30 days at 37°C. Data are presented as average ± SD of 3 independent batches.

Efficiency of particle association with DC was studied by culturing DC in the presence of the 3 different particle formulations at 4ºC (binding) and 37ºC (binding & internalization) with various concentrations of encapsulated Ag. DC showed very high capacity to bind and internalize NP compared to MP (**Figure 2A**), and we observed consistently that both NP 50:50 and 75:25 were engulfed with higher efficiency than MP (**Figure 2B & C**). In line with these results, we have recently shown that NP are internalized by $CD11c^+$ DC *in vivo* at the site of injection [52]. Internalized NP function as an intracellular Ag depot gradually releasing the encapsulated Ag into MHC class I processing and cross presentation pathways, leading to sustained intracellular release [12, 53].

In contrast, MP are poorly internalized, likely because of their large size at the early phases of PLGA degradation, releasing the encapsulated Ag and TLRL locally via an initial burst followed by a more gradual release due to polymer hydrolysis (**Figure 1**). Consequently, MP essentially deliver soluble Ag and TLRL to DC and function as a local Ag depot under the skin at the site of injection. We and others have previously shown that DC poorly cross-present protein Ag when it is delivered in soluble form [9, 10]. Therefore, if the aim is to induce a robust $CD8^+$ T cell response through vaccination, micron-sized particulate vaccines might not be the right candidates.

MHC class I Ag cross-presentation by DC of OVA encapsulated in NP or in MP was studied *in vitro*. Soluble OVA is poorly cross-presented in MHC class I processing routes, unless very high amounts are added to DC cultures [9]. We observed that NP performed 8 - 10 fold better compared to MP in routing Ag into MHC class I processing pathways, whereas NP 50:50 and NP 75:25 showed similar efficiency, possibly due to the similar release kinetics at early time-points (**Figure 3A**). $CD8^+$ T cell activation was calculated relative to that induced by 5 nM SIINFEKL as 100%, and no Ag as baseline

(see **Figure 3B** for raw data). Our observations are supported by the report of Joshi et al., who observed that the efficiency of particle uptake and upregulation of MHC class I and CD86 expression on BMDC was correlated with small particle size [31].

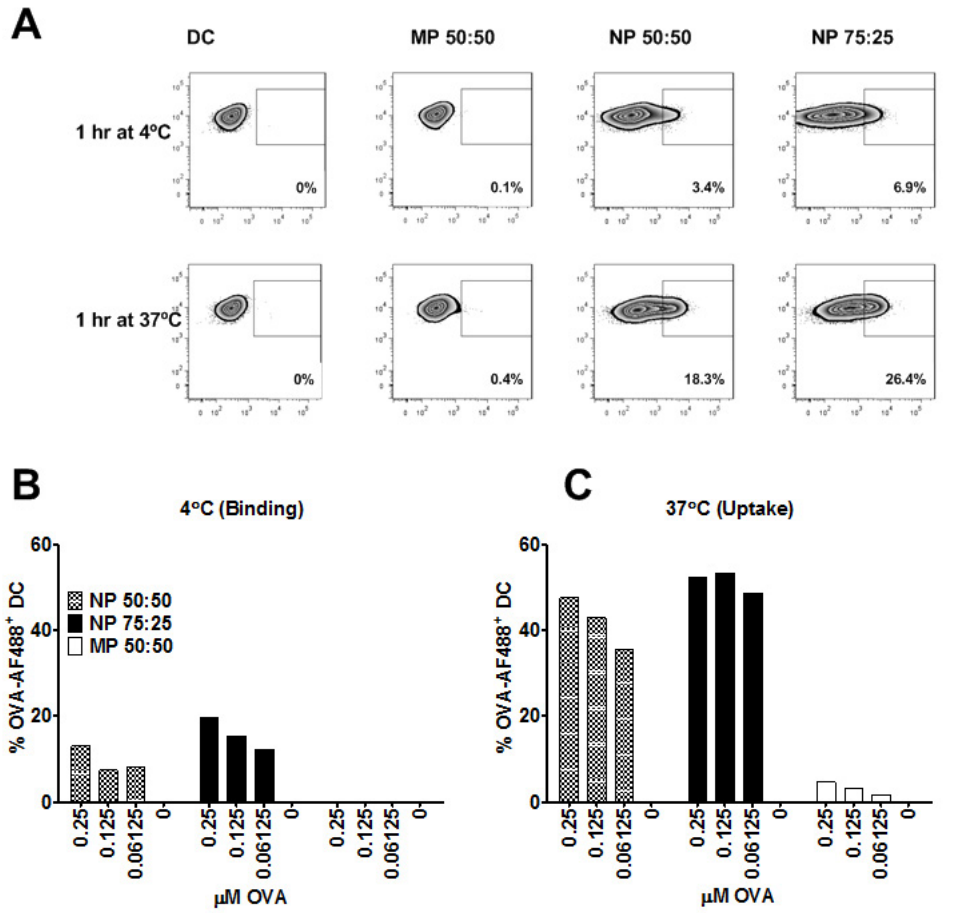

Figure2: Binding and uptake of NP-encapsulated protein Ag by dendritic cells compared to MP-encapsulated Ag. A) D1 dendritic cells cells were incubated for 1 h with titrated amounts (µM) of OVA (and poly(I:C)) encapsulated in NP 50:50, NP 75:25 and MP 50:50 also containing OVA-AF488 dye. Ag incubation with DC was performed in parallel at **B)** 4°C (binding) and **C)** 37°C (binding & internalization), followed by extensive washing to remove unbound Ag and cell fixation with 4% paraformaldehyde. Cells were analyzed by flow cytometry to determine green fluorescence. Percentages of DC positive for OVA-AF488 were quantified at different Ag concentrations. Data shown are measurements from one experiment.

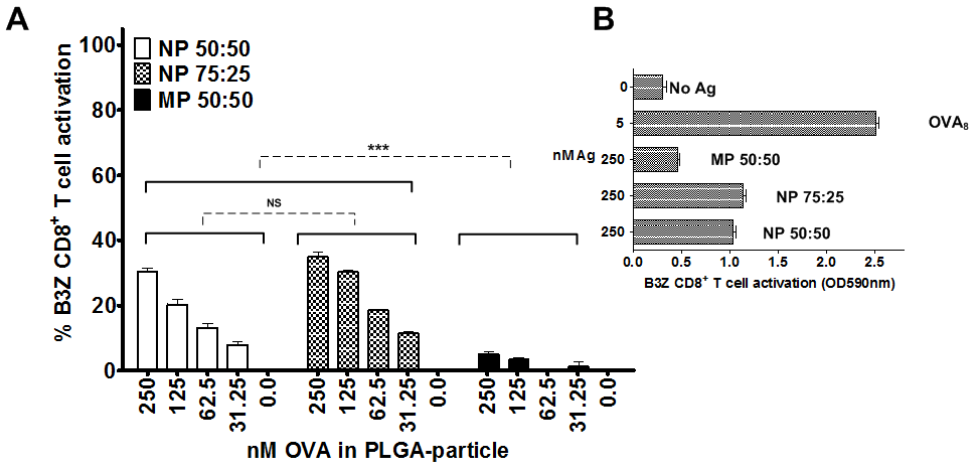

Figure3: Efficient MHC class I cross-presentation of protein Ag incorporated in NP but not MP. A) D1 cells were pulsed for 2 h with titrated amounts (nM) of OVA (and poly(I:C)) encapsulated in NP 50:50, NP 75:25 or MP 50:50. MHC class I presentation of processed OVA protein antigen was detected by co-culture with H-2Kb/SIINFEKL-specific B3Z CD8+ T cells. Normalized values in panel A were calculated based on the OD590nm values obtained by using DC loaded with SIINFEKL cultured together with B3Z CD8+ T cells (OD590nm = 2.53 = 100% CD8+ T cell activation). **B)** OD590nm values obtained with the highest concentration of OVA (250 nM) (and poly(I:C)) encapsulated NP 50:50, NP 75:25, MP 50:50 or SIINFEKL (5 nM, known to result in maximal CD8+ T cell activation in this assay). Data shown are means of triplicate measurements ± SD as % from one representative example out of at least three independent experiments.

We subsequently analyzed whether the enhanced MHC class I presentation observed *in vitro* would translate into better CD8+ T cell priming *in vivo*. For this purpose, we vaccinated animals with NP and MP formulations encapsulating OVA and Poly(I:C) or Ag and adjuvant formulated in IFA. Mice were sacrificed 7 days later to determine the number of Ag-specific CD8+ T cells in the spleen. Since NP 50:50 showed similar CD8+ T cell priming *in vivo* as NP 75:25 (data not shown), the ensuing *in vivo* studies comparing NP and MP were performed based on particle formulations using the same polymer composition (PLGA 50:50).

The *in vivo* vaccine potency of NP and MP formulations was analyzed in comparison to IFA. It is well known that plain PLGA particles have poor immune-activating properties: the absence of TLRL in PLGA-based vaccine protocols results in defective immune activation [8, 24, 54]. For that reason poly(I:C) was co-encapsulated with the Ag in our particles to achieve a strong activation of DC and promote the production of IL-12 [9]. Vaccinations with NP led to considerably higher numbers of Ag-specific CD8+ T cells compared to MP ($p = 0.01$) and IFA ($p = 0.04$), with almost no difference being observed between vaccination with MP and non-vaccinated mice (Figure 4). NP also performed better than IFA, suggesting that internalization of the particles may be of importance in inducing a stronger cellular immune response in comparison to sustained release from a local Ag depot, though the mechanisms by which IFA delivers Ag are still not fully understood.

Analysis of cytokine production showed that vaccination with NP resulted in the highest production of IFN-γ (**Supplemental Figure 5**) but did not induce much IL-2 (data not shown). Under these conditions we also analyzed the $CD8^+$ T cell *in vivo* cytotoxicity. In line with the relatively higher number of specific $CD8^+$ T cells induced with NP, animals vaccinated with NP showed effective OVA-specific cytotoxicity *in vivo* (**Supplemental Figure 6**).

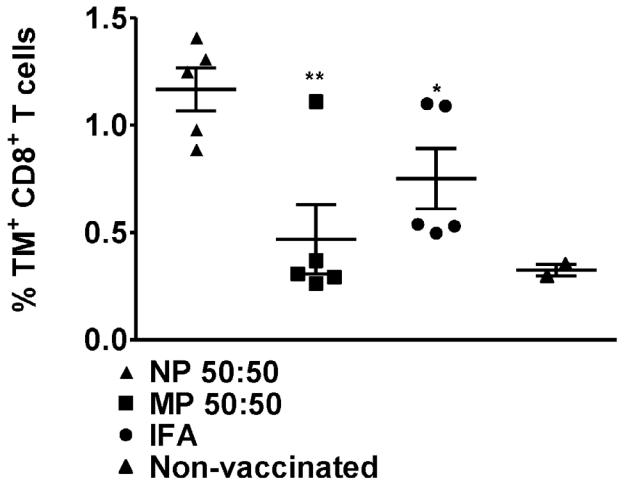

Figure 4: NP vaccine shows effective $CD8^+$ T cell priming potency. Naïve animals received a single s.c. vaccination with the 50 µg OVA and 20 µg poly(I:C) formulated in NP 50:50 (closed triangles), MP 50:50 (open squares) or in IFA (closed circles). Non-vaccinated animals were used as control (open triangles). Mice were sacrificed on day 7 after vaccination and the % of SIINFEKL-TM^+ $CD8^+$ T cells were measured by flow cytometry. Results shown are representative of one experiment out of two and present averages ± SEM from n = 3 - 5 mice per group, * = $p < 0.05$ and ** = $p < 0.01$ using an unpaired student t test in relation to the group immunized with NP 50:50. Each symbol represents the specific T cell response in an individual mouse.

Co-encapsulation of OVA and TLRL has previously shown to induce anti-OVA (IgG) humoral responses, as well as polarization of the immune response [24, 37, 55]. Blood samples were collected on day 21 or 35 after vaccination and titers of IgG1, IgG2a and IgG2b antibodies were determined. NP and IFA, but not MP, induced IgG1 production and low titers of IgG2a and IgG2b after single vaccination (prime) (**Figure 5A** & **B** & **C)**. A second vaccination (boost) considerably enhanced the IgG1 titers for IFA and NP, but again not MP (**Figure 5D**). Significant IgG2a titers were induced after boost with NP but poorly by the other vaccines (**Figure 5E**). IgG2b titers were induced to a similar level by vaccinations with IFA and NP (**Figure 5F**).

IgG2a is the IgG-subtype associated with TH1 responses in mice and analysis of the IgG1/IgG2a ratio allows one to determine the immune-polarization [56]. Vaccinations with NP resulted in a more balanced TH1/TH2 antibody response characterized by similar titers of IgG1 and IgG2a (IgG1/IgG2a ≈ 1).

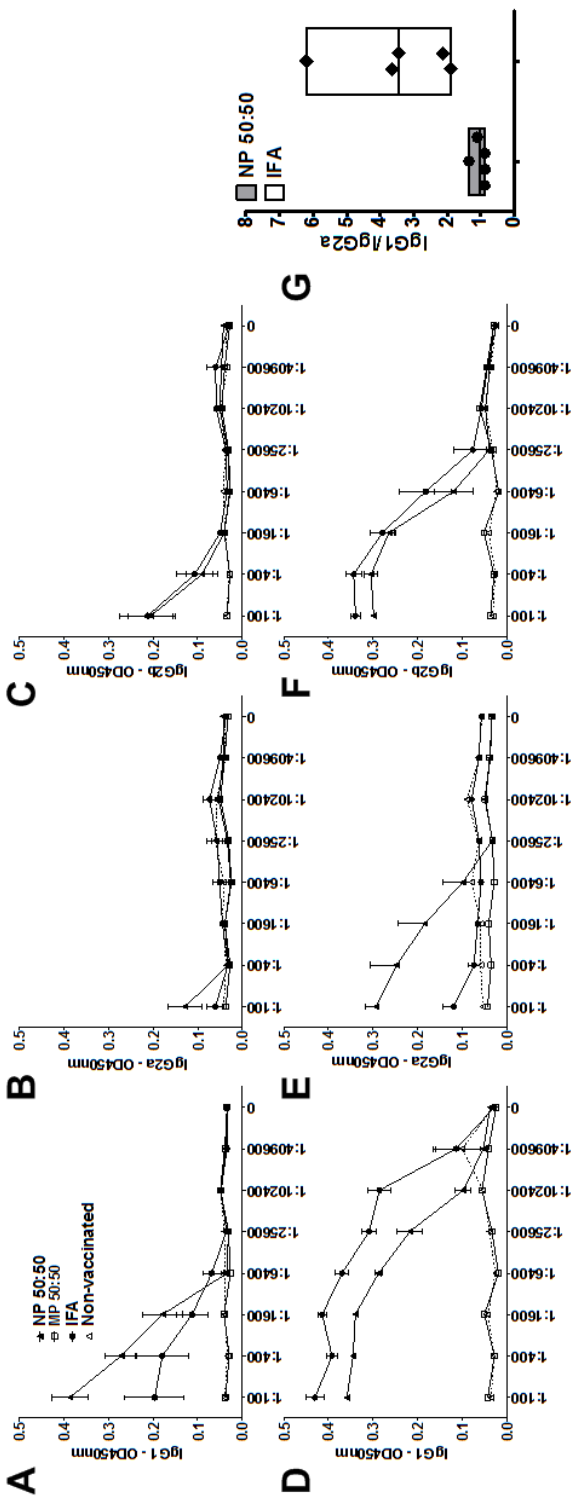

Figure 5: Induction of balanced TH1/TH2-associated humoral responses by vaccinations with NP. A) Animals were vaccinated on day 0 and day 28 with 50 µg OVA and 20 µg poly(I:C) formulated in NP 50:50 (closed triangles), MP 50:50 (open squares) or in IFA (closed circles). Non-vaccinated animals were used as control (open triangles). Serum samples were collected on day 21 (3 weeks after prime, panel **A, B** and **C)** and 35 (1 week after boost, panel **D, E** and **F)** and the titers for IgG1, IgG2a and IgG2b determined via ELISA. G) Immune polarization was calculated for NP 50:50 (closed circles) and IFA (closed diamonds) based on the IgG1/IgG2a ratio determining ([IgG1 OD450nm vaccinated mice/OD450nm non-immunize mice]/[IgG2a OD450nm vaccinated mice/OD450nm non-immunized mice]) at the lowest serum dilution (1:100). Results shown are averages ± SEM from 5 mice per group and time-point, * = $p < 0.05$, ** = $p < 0.01$ and *** = $p < 0.01$ two-way ANOVA with Bonferroni post tests.

In contrast, vaccinations with IFA led to a predominant TH2 response (IgG1/IgG2a > 2) (**Figure 5G**), which might contribute to the differences in $CD8^+$ T cell responses detected after vaccinations. A predominant humoral TH2 response will likely be accompanied by a weak $CD8^+$ T cell response [57]. The higher production of IgG2a after vaccination is linked to the increased uptake by DC of particles encapsulating the protein and adjuvant [31], compared to soluble protein and poly(I:C). In addition, direct stimulation of B cells by the NP might also contribute better IgG2a responses compared to IFA-based vaccine formulations [21, 58].

PLGA MP are reported to have a negative effect on protein structural integrity, leading to denaturation and aggregation [59]. Differences in Ag integrity of OVA in NP compared to OVA in MP might also play a role in the immune responses we report here, since a larger and deeper inner core of MP likely results in more extensive local acidification as compared to the much smaller NP [60]. However, release of denatured OVA from MP should induce at least equal but probably stronger *in vivo* T cell [61] and B cell responses [62, 63] compared to native OVA. In support of this we have shown that proteolytic cleavage of whole proteins into smaller peptide strands improves the activation of T cells by human DC [64]. Still, we cannot exclude that the inability of MPs to induce antibodies cross-reacting with native OVA may be due in part to a more dramatic loss of protein structure compared to the NP.

4. Conclusions

Our results show that the ability of DC to internalize Ag- and TLRL-containing PLGA particles is a crucial factor to achieve effective MHC class I cross-presentation, prime $CD8^+$ T cells and to elicit both a T and B cell response after direct vaccinations. We report here that NP are more efficiently internalized by DC *in vitro*, resulting in superior vaccine potency compared to MP when aiming to stimulate cellular immune responses. Furthermore, NP co-encapsulating Ag and TLRL outperformed IFA as an adjuvant, by more efficiently boosting $CD8^+$ T cell activation and (IgG2a) antibody production. In conclusion, because of the superior responses induced in comparison to IFA, our data supports the application of biodegradable PLGA NP delivery systems as a substitute for mineral oil emulsions for protein vaccine-based immunotherapy.

Acknowledgements

The authors thank Ahmed Allam and Amir Ghassemi for the contribution to particle formulation studies, and Reza Nejadnik for support in particle characterization. This study was supported by grants from Immune System Activation (ISA) Pharmaceuticals and the Leiden University Medical Center.

Conflict of Interest

The authors declare that they have no conflict of interest.

5. References

1. Ada, G., Overview of vaccines and vaccination. Mol Biotechnol, 2005. 29(3): p. 255-72.
2. Arens, R., T. van Hall, S.H. van der Burg, F. Ossendorp, and C.J. Melief, Prospects of combinatorial synthetic peptide vaccine-based immunotherapy against cancer. Semin Immunol, 2013. 25(2): p. 182-90.
3. Melief, C.J., Cancer immunotherapy by dendritic cells. Immunity, 2008. 29(3): p. 372-83.
4. Waeckerle-Men, Y., E.U. Allmen, B. Gander, E. Scandella, E. Schlosser, G. Schmidtke, H.P. Merkle, and M. Groettrup, Encapsulation of proteins and peptides into biodegradable poly(D,L-lactide-co-glycolide) microspheres prolongs and enhances antigen presentation by human dendritic cells. Vaccine, 2006. 24(11): p. 1847-57.
5. Kenter, G.G., M.J. Welters, A.R. Valentijn, M.J. Lowik, D.M. Berends-van der Meer, A.P. Vloon, F. Essahsah, L.M. Fathers, R. Offringa, J.W. Drijfhout, A.R. Wafelman, J. Oostendorp, G.J. Fleuren, S.H. van der Burg, and C.J. Melief, Vaccination against HPV-16 oncoproteins for vulvar intraepithelial neoplasia. N Engl J Med, 2009. 361(19): p. 1838-47.
6. Atanackovic, D., N.K. Altorki, E. Stockert, B. Williamson, A.A. Jungbluth, E. Ritter, D. Santiago, C.A. Ferrara, M. Matsuo, A. Selvakumar, B. Dupont, Y.T. Chen, E.W. Hoffman, G. Ritter, L.J. Old, and S. Gnjatic, Vaccine-induced $CD4^+$ T cell responses to MAGE-3 protein in lung cancer patients. J Immunol, 2004. 172(5): p. 3289-96.
7. Heit, A., F. Schmitz, T. Haas, D.H. Busch, and H. Wagner, Antigen co-encapsulated with adjuvants efficiently drive protective T cell immunity. Eur J Immunol, 2007. 37(8): p. 2063-74.
8. Schlosser, E., M. Mueller, S. Fischer, S. Basta, D.H. Busch, B. Gander, and M. Groettrup, TLR ligands and antigen need to be coencapsulated into the same biodegradable microsphere for the generation of potent cytotoxic T lymphocyte responses. Vaccine, 2008. 26(13): p. 1626-37.
9. Rosalia, R.A., A.L. Silva, M. Camps, A. Allam, W. Jiskoot, S.H. van der Burg, F. Ossendorp, and J. Oostendorp, Efficient ex vivo induction of T cells with potent anti-tumor activity by protein antigen encapsulated in nanoparticles. Cancer Immunol Immunother, 2013. 62(7): p. 1161-73.
10. Braun, M., C. Jandus, P. Maurer, A. Hammann-Haenni, K. Schwarz, M.F. Bachmann, D.E. Speiser, and P. Romero, Virus-like particles induce robust human T-helper cell responses. Eur J Immunol, 2012. 42(2): p. 330-40.
11. Rosalia, R.A., L.J. Cruz, S. van Duikeren, A.T. Tromp, A.L. Silva, W. Jiskoot, T. de Gruijl, C. Lowik, J. Oostendorp, S.H. van der Burg, and F. Ossendorp, CD40-targeted dendritic cell delivery of PLGA-nanoparticle vaccines induce potent anti-tumor responses. Biomaterials, 2014.
12. Shen, H., A.L. Ackerman, V. Cody, A. Giodini, E.R. Hinson, P. Cresswell, R.L. Edelson, W.M. Saltzman, and D.J. Hanlon, Enhanced and prolonged cross-presentation following endosomal escape of exogenous antigens encapsulated in biodegradable nanoparticles. Immunology, 2006. 117(1): p. 78-88.

13. Tran, K.K., X. Zhan, and H. Shen, Polymer blend particles with defined compositions for targeting antigen to both class I and II antigen presentation pathways. Adv Healthc Mater, 2014. 3(5): p. 690-702.
14. Tacken, P.J., I.J. de Vries, R. Torensma, and C.G. Figdor, Dendritic-cell immunotherapy: from ex vivo loading to *in vivo* targeting. Nat Rev Immunol, 2007. 7(10): p. 790-802.
15. Hailemichael, Y., Z. Dai, N. Jaffarzad, Y. Ye, M.A. Medina, X.F. Huang, S.M. Dorta-Estremera, N.R. Greeley, G. Nitti, W. Peng, C. Liu, Y. Lou, Z. Wang, W. Ma, B. Rabinovich, R.T. Sowell, K.S. Schluns, R.E. Davis, P. Hwu, and W.W. Overwijk, Persistent antigen at vaccination sites induces tumor-specific CD8(+) T cell sequestration, dysfunction and deletion. Nat Med., 2013. 19(4): p. 465-72. doi: 10.1038/nm.3105. Epub 2013 Mar 3.
16. Parker, R., S. Deville, L. Dupuis, F. Bertrand, and J. Aucouturier, Adjuvant formulation for veterinary vaccines: Montanide™ Gel safety profile. Procedia in Vaccinology, 2009. 1(1): p. 140-147.
17. Mueller, M., E. Schlosser, B. Gander, and M. Groettrup, Tumor eradication by immunotherapy with biodegradable PLGA microspheres--an alternative to incomplete Freund's adjuvant. Int J Cancer, 2011. 129(2): p. 407-16.
18. Mundargi, R.C., V.R. Babu, V. Rangaswamy, P. Patel, and T.M. Aminabhavi, Nano/micro technologies for delivering macromolecular therapeutics using poly(D,L-lactide-co-glycolide) and its derivatives. J Control Release, 2008. 125(3): p. 193-209.
19. Newman, K.D., P. Elamanchili, G.S. Kwon, and J. Samuel, Uptake of poly(D,L-lactic-co-glycolic acid) microspheres by antigen-presenting cells *in vivo*. J Biomed Mater Res, 2002. 60(3): p. 480-6.
20. Putney, S.D. and P.A. Burke, Improving protein therapeutics with sustained-release formulations. Nat Biotechnol, 1998. 16(2): p. 153-7.
21. Kasturi, S.P., I. Skountzou, R.A. Albrecht, D. Koutsonanos, T. Hua, H.I. Nakaya, R. Ravindran, S. Stewart, M. Alam, M. Kwissa, F. Villinger, N. Murthy, J. Steel, J. Jacob, R.J. Hogan, A. Garcia-Sastre, R. Compans, and B. Pulendran, Programming the magnitude and persistence of antibody responses with innate immunity. Nature, 2011. 470(7335): p. 543-7.
22. Badiee, A., N. Davies, K. McDonald, K. Radford, H. Michiue, D. Hart, and M. Kato, Enhanced delivery of immunoliposomes to human dendritic cells by targeting the multilectin receptor DEC-205. Vaccine, 2007. 25(25): p. 4757-66.
23. Zhang, X.Q., C.E. Dahle, N.K. Baman, N. Rich, G.J. Weiner, and A.K. Salem, Potent antigen-specific immune responses stimulated by codelivery of CpG ODN and antigens in degradable microparticles. J Immunother, 2007. 30(5): p. 469-78.
24. Pulendran, B. and R. Ahmed, Immunological mechanisms of vaccination. Nat Immunol, 2011. 12(6): p. 509-17.
25. Demento, S.L., N. Bonafe, W. Cui, S.M. Kaech, M.J. Caplan, E. Fikrig, M. Ledizet, and T.M. Fahmy, TLR9-targeted biodegradable nanoparticles as immunization vectors protect against West Nile encephalitis. J Immunol, 2010. 185(5): p. 2989-97.
26. Link, A., F. Zabel, Y. Schnetzler, A. Titz, F. Brombacher, and M.F. Bachmann, Innate immunity mediates follicular transport of particulate but not soluble

protein antigen. J Immunol, 2012. 188(8): p. 3724-33.
27. Johansen, P., T. Storni, L. Rettig, Z. Qiu, A. Der-Sarkissian, K.A. Smith, V. Manolova, K.S. Lang, G. Senti, B. Mullhaupt, T. Gerlach, R.F. Speck, A. Bot, and T.M. Kundig, Antigen kinetics determines immune reactivity. Proc Natl Acad Sci U S A, 2008. 105(13): p. 5189-94.
28. Simon, L.C. and C.M. Sabliov, The effect of nanoparticle properties, detection method, delivery route and animal model on poly(lactic-co-glycolic) acid nanoparticles biodistribution in mice and rats. Drug Metab Rev, 2013.
29. Oyewumi, M.O., A. Kumar, and Z. Cui, Nano-microparticles as immune adjuvants: correlating particle sizes and the resultant immune responses. Expert Rev Vaccines, 2010. 9(9): p. 1095-107.
30. Jain, S., P. Malyala, M. Pallaoro, M. Giuliani, H. Petersen, D.T. O'Hagan, and M. Singh, A two-stage strategy for sterilization of poly(lactide-co-glycolide) particles by gamma-irradiation does not impair their potency for vaccine delivery. J Pharm Sci, 2011. 100(2): p. 646-54.
31. Joshi, V.B., S.M. Geary, and A.K. Salem, Biodegradable particles as vaccine delivery systems: size matters. AAPS J, 2013. 15(1): p. 85-94.
32. Tran, K.K. and H. Shen, The role of phagosomal pH on the size-dependent efficiency of cross-presentation by dendritic cells. Biomaterials, 2009. 30(7): p. 1356-62.
33. Winzler, C., P. Rovere, M. Rescigno, F. Granucci, G. Penna, L. Adorini, V.S. Zimmermann, J. Davoust, and P. Ricciardi-Castagnoli, Maturation stages of mouse dendritic cells in growth factor-dependent long-term cultures. J Exp Med, 1997. 185(2): p. 317-28.
34. Schuurhuis, D.H., A. Ioan-Facsinay, B. Nagelkerken, J.J. van Schip, C. Sedlik, C.J. Melief, J.S. Verbeek, and F. Ossendorp, Antigen-antibody immune complexes empower dendritic cells to efficiently prime specific $CD8^+$ CTL responses *in vivo*. J Immunol, 2002. 168(5): p. 2240-6.
35. Sanderson, S. and N. Shastri, LacZ inducible, antigen/MHC-specific T cell hybrids. Int Immunol, 1994. 6(3): p. 369-76.
36. Rosalia, R.A., A.L. Silva, M. Camps, A. Allam, W. Jiskoot, S.H. van der Burg, F. Ossendorp, and J. Oostendorp, Efficient ex vivo induction of T cells with potent anti-tumor activity by protein antigen encapsulated in nanoparticles. Cancer immunology, immunotherapy : CII, 2013.
37. Slutter, B., S. Bal, C. Keijzer, R. Mallants, N. Hagenaars, I. Que, E. Kaijzel, W. van Eden, P. Augustijns, C. Lowik, J. Bouwstra, F. Broere, and W. Jiskoot, Nasal vaccination with N-trimethyl chitosan and PLGA based nanoparticles: nanoparticle characteristics determine quality and strength of the antibody response in mice against the encapsulated antigen. Vaccine, 2010. 28(38): p. 6282-91.
38. Sah, H., A new strategy to determine the actual protein content of poly(lactide-co-glycolide) microspheres. J Pharm Sci, 1997. 86(11): p. 1315-8.
39. Silva, A.L., R.A. Rosalia, A. Sazak, M.G. Carstens, F. Ossendorp, J. Oostendorp, and W. Jiskoot, Optimization of encapsulation of a synthetic long peptide in PLGA nanoparticles: low-burst release is crucial for efficient $CD8^{(+)}$ T cell activation. Eur J Pharm Biopharm, 2013. 83(3): p. 338-45.
40. Kreutz, M., P.J. Tacken, and C.G. Figdor, Targeting dendritic cells--why bother?

Blood, 2013. 121(15): p. 2836-44.
41. Schliehe, C., C. Redaelli, S. Engelhardt, M. Fehlings, M. Mueller, N. van Rooijen, M. Thiry, K. Hildner, H. Weller, and M. Groettrup, CD8- dendritic cells and macrophages cross-present poly(D,L-lactate-co-glycolate) acid microsphere-encapsulated antigen *in vivo*. J Immunol, 2011. 187(5): p. 2112-21.
42. Fifis, T., A. Gamvrellis, B. Crimeen-Irwin, G.A. Pietersz, J. Li, P.L. Mottram, I.F. McKenzie, and M. Plebanski, Size-dependent immunogenicity: therapeutic and protective properties of nano-vaccines against tumors. J Immunol, 2004. 173(5): p. 3148-54.
43. Gutierro, I., R.M. Hernandez, M. Igartua, A.R. Gascon, and J.L. Pedraz, Size dependent immune response after subcutaneous, oral and intranasal administration of BSA loaded nanospheres. Vaccine, 2002. 21(1-2): p. 67-77.
44. Demento, S.L., W. Cui, J.M. Criscione, E. Stern, J. Tulipan, S.M. Kaech, and T.M. Fahmy, Role of sustained antigen release from nanoparticle vaccines in shaping the T cell memory phenotype. Biomaterials, 2012. 33(19): p. 4957-64.
45. Xiang, S.D., A. Scholzen, G. Minigo, C. David, V. Apostolopoulos, P.L. Mottram, and M. Plebanski, Pathogen recognition and development of particulate vaccines: does size matter? Methods, 2006. 40(1): p. 1-9.
46. Sharp, F.A., D. Ruane, B. Claass, E. Creagh, J. Harris, P. Malyala, M. Singh, D.T. O'Hagan, V. Petrilli, J. Tschopp, L.A. O'Neill, and E.C. Lavelle, Uptake of particulate vaccine adjuvants by dendritic cells activates the NALP3 inflammasome. Proc Natl Acad Sci U S A, 2009. 106(3): p. 870-5.
47. Mata, E., M. Igartua, R.M. Hernandez, J.E. Rosas, M.E. Patarroyo, and J.L. Pedraz, Comparison of the adjuvanticity of two different delivery systems on the induction of humoral and cellular responses to synthetic peptides. Drug Deliv, 2010. 17(7): p. 490-9.
48. Zeestraten, E.C., F.M. Speetjens, M.J. Welters, S. Saadatmand, L.F. Stynenbosch, R. Jongen, E. Kapiteijn, H. Gelderblom, H.W. Nijman, A.R. Valentijn, J. Oostendorp, L.M. Fathers, J.W. Drijfhout, C.J. van de Velde, P.J. Kuppen, S.H. van der Burg, and C.J. Melief, Addition of interferon-alpha to the p53-SLP(R) vaccine results in increased production of interferon-gamma in vaccinated colorectal cancer patients: a phase I/II clinical trial. Int J Cancer, 2013. 132(7): p. 1581-91.
49. Yeo, Y. and K. Park, Control of encapsulation efficiency and initial burst in polymeric microparticle systems. Arch Pharm Res, 2004. 27(1): p. 1-12.
50. Leelarasamee, N., S.A. Howard, C.J. Malanga, L.A. Luzzi, T.F. Hogan, S.J. Kandzari, and J.K. Ma, Kinetics of drug release from polylactic acid-hydrocortisone microcapsules. J Microencapsul, 1986. 3(3): p. 171-9.
51. Mansour, H.M., M. Sohn, A. Al-Ghananeem, and P.P. Deluca, Materials for pharmaceutical dosage forms: molecular pharmaceutics and controlled release drug delivery aspects. Int J Mol Sci, 2010. 11(9): p. 3298-322.
52. Cruz, L.J., R.A. Rosalia, J.W. Kleinovink, F. Rueda, C.W. Lowik, and F. Ossendorp, Targeting nanoparticles to CD40, DEC-205 or CD11c molecules on dendritic cells for efficient CD8 T cell response: A comparative study. J Control Release, 2014. 192C: p. 209-218.
53. Cruz, L.J., P.J. Tacken, R. Fokkink, B. Joosten, M.C. Stuart, F. Albericio, R. Torensma, and C.G. Figdor, Targeted PLGA nano- but not microparticles

specifically deliver antigen to human dendritic cells via DC-SIGN *in vitro*. J Control Release, 2010. 144(2): p. 118-26.
54. Fischer, S., E. Schlosser, M. Mueller, N. Csaba, H.P. Merkle, M. Groettrup, and B. Gander, Concomitant delivery of a CTL-restricted peptide antigen and CpG ODN by PLGA microparticles induces cellular immune response. J Drug Target, 2009. 17(8): p. 652-61.
55. Krishnamachari, Y. and A.K. Salem, Innovative strategies for co-delivering antigens and CpG oligonucleotides. Adv Drug Deliv Rev, 2009. 61(3): p. 205-17.
56. Finkelman, F.D., J. Holmes, I.M. Katona, J.F. Urban, Jr., M.P. Beckmann, L.S. Park, K.A. Schooley, R.L. Coffman, T.R. Mosmann, and W.E. Paul, Lymphokine control of *in vivo* immunoglobulin isotype selection. Annu Rev Immunol, 1990. 8: p. 303-33.
57. Romagnani, S., Th1/Th2 cells. Inflamm Bowel Dis, 1999. 5(4): p. 285-94.
58. Eckl-Dorna, J. and F.D. Batista, BCR-mediated uptake of antigen linked to TLR9 ligand stimulates B-cell proliferation and antigen-specific plasma cell formation. Blood, 2009. 113(17): p. 3969-77.
59. van de Weert, M., W.E. Hennink, and W. Jiskoot, Protein instability in poly(lactic-co-glycolic acid) microparticles. Pharm Res, 2000. 17(10): p. 1159-67.
60. Samadi, N., A. Abbadessa, A. Di Stefano, C.F. van Nostrum, T. Vermonden, S. Rahimian, E.A. Teunissen, M.J. van Steenbergen, M. Amidi, and W.E. Hennink, The effect of lauryl capping group on protein release and degradation of poly(D,L-lactic-co-glycolic acid) particles. J Control Release, 2013. 172(2): p. 436-43.
61. Schirmbeck, R., W. Bohm, and J. Reimann, Injection of detergent-denaturd ovalbumin primes murine class I-restricted cytotoxic T cells in vivo. Eur J Immunol, 1994. 24(9): p. 2068-72.
62. Huang, C.F., T.C. Wu, Y.H. Chu, K.S. Hwang, C.C. Wang, and H.J. Peng, Effect of neonatal sublingual vaccination with native or denatured ovalbumin and adjuvant CpG or cholera toxin on systemic and mucosal immunity in mice. Scand J Immunol, 2008. 68(5): p. 502-10.
63. Peng, H.J., Z.N. Chang, L.C. Tsai, S.N. Su, H.D. Shen, and C.H. Chang, Heat denaturation of egg-white proteins abrogates the induction of oral tolerance of specific Th2 immune responses in mice. Scand J Immunol, 1998. 48(5): p. 491-6.
64. Rosalia, R.A., E.D. Quakkelaar, A. Redeker, S. Khan, M. Camps, J.W. Drijfhout, A.L. Silva, W. Jiskoot, T. van Hall, P.A. van Veelen, G. Janssen, K. Franken, L.J. Cruz, A. Tromp, J. Oostendorp, S.H. van der Burg, F. Ossendorp, and C.J. Melief, Dendritic cells process synthetic long peptides better than whole protein, improving antigen presentation and T-cell activation. Eur J Immunol, 2013. 43(10): p. 2554-65.

Supplemental Material

Supplemental Table 1: Protein concentration of sample from the last day of release study (day 40). Protein concentration was measured by BCA assay and by fluorescence in supernatants (SN) and expressed as percentage of total encapsulated OVA.

Particles	BCA Assay (% in SN)	Fluorescence (% in SN)
NP 50:50	82 ± 14	85 ±14
NP 75:25	53 ± 10	52 ± 9
MP 50:50	48 ± 10	40 ± 3

Supplemental Table 2: Distribution of MP diameters (µm) determined by LO before (BF) and after filtration (AF) in terms of percentage of total number and volume. Mean values are presented in the last row.

	% Number		% Volume	
Diameter (µm)	BF	AF	BF	AF
1-2	33.2 ± 6.7	39.0 ± 11.0	0.0 ± 0.0	0.0 ± 0.0
2-5	38.6 ± 7.1	16.9 ± 2.9	0.5 ± 0.3	0.0 ± 0.0
5-10	21.2 ± 3.0	10.5 ± 5.4	2.4 ± 1.4	0.1 ± 0.1
10-15	3.7 ± 2.1	4.3 ± 3.2	1.7 ± 1.2	0.1 ± 0.1
15-20	1.3 ± 1.0	4.0 ± 3.1	1.4 ± 1.1	0.4 ± 0.3
20-25	0.6 ± 0.6	4.1 ± 2.7	1.1 ± 0.8	0.8 ± 0.7
25-30	0.3 ± 0.4	3.2 ± 1.7	1.2 ± 0.9	1.2 ± 0.9
30-40	0.4 ± 0.5	4.8 ± 0.1	2.3 ± 1.4	3.2 ± 2.1
40-50	0.2 ± 0.2	3.4 ± 0.6	2.7 ± 0.9	5.0 ± 3.5
50-60	0.1 ± 0.1	2.4 ± 0.3	2.5 ± 1.4	5.9 ± 3.8
60-75	0.1 ± 0.1	2.2 ± 0.3	6.0 ± 1.9	10.6 ± 7.6
75-100	0.2 ± 0.2	2.4 ± 1.2	17.1 ± 3.7	19.3 ± 8.5
100-125	0.1 ± 0.1	1.4 ± 1.5	20.4 ± 4.3	15.3 ± 2.7
125-150	0.0 ± 0.0	0.6 ± 0.8	11.8 ± 5.7	10.0 ± 5.9
150-200	0.0 ± 0.0	0.8 ± 1.1	29.0 ± 17.1	28.2 ± 18.1
Mean diameter	5 ± 1.0	17 ± 5.0	114 ± 16.0	112 ± 26.0

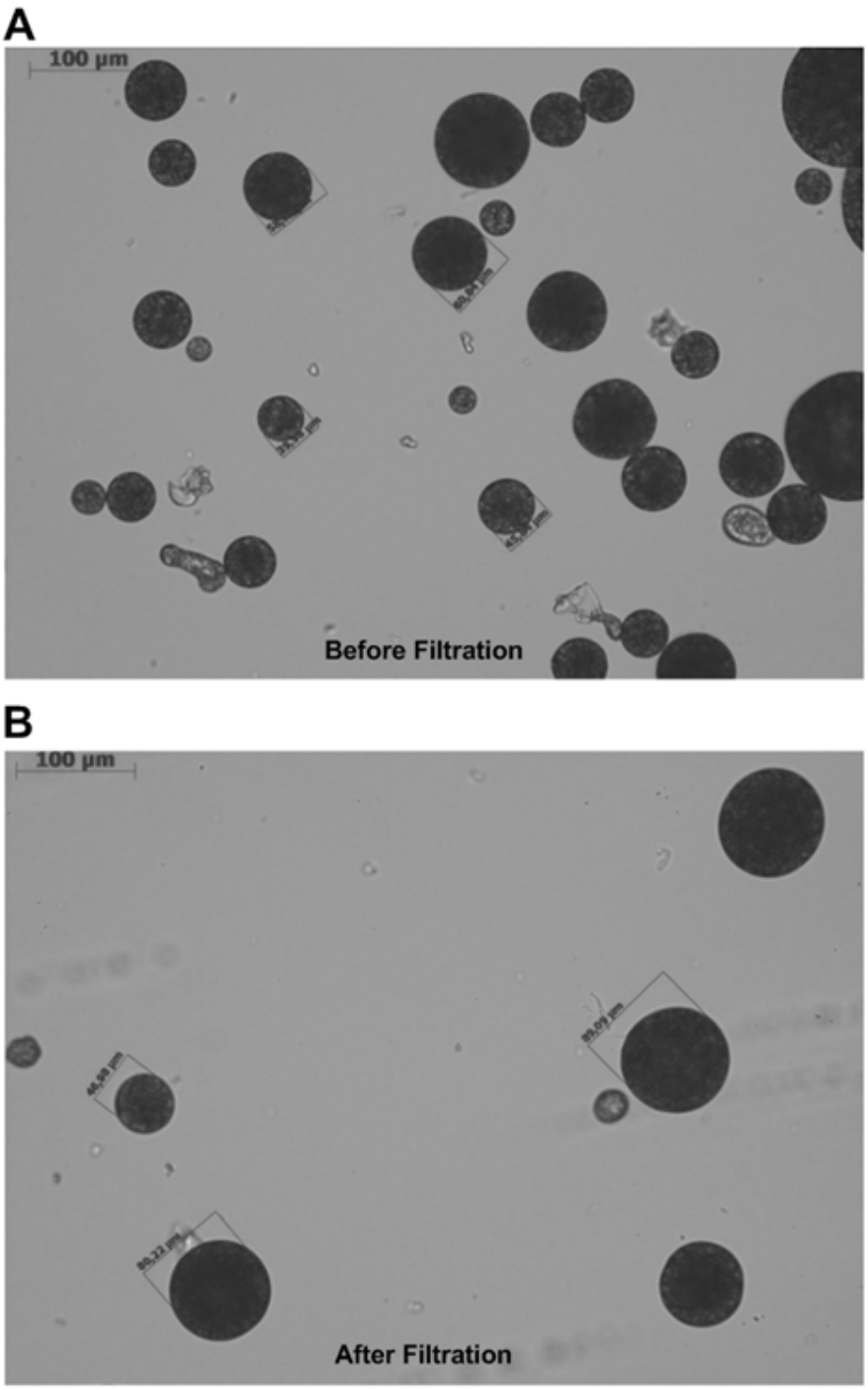

Supplemental Figure 1: Representative images of MP preparations analyzed by optical microscopy (20x magnification) before and after stirred-cell filtration.

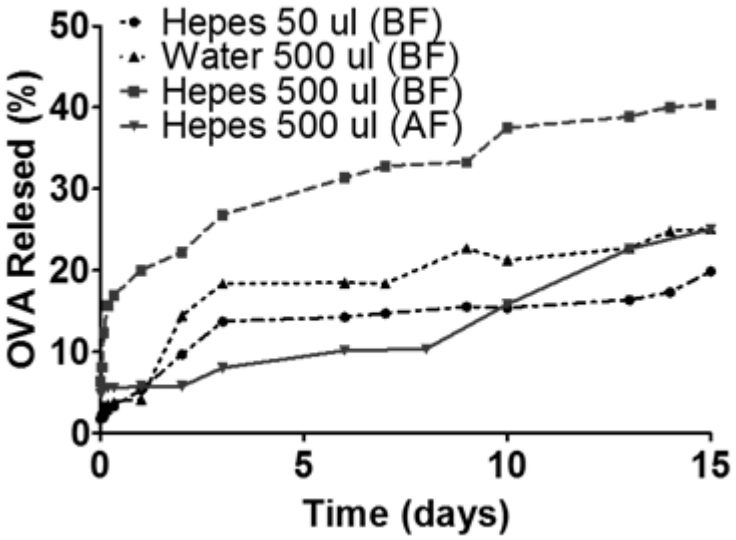

Supplemental Figure 2: OVA release after filtration (AF) and before filtration (BF) of MP with different inner phase composition using PLGA 50:50 observed for 15 days. Hepes 50 µl (BF) (open diamonds) corresponds to an inner phase of 50 µl of 20 mg/ml OVA solution in 25 mM Hepes pH 7.4; and Water 500 µl (BF) (open triangles) to an inner phase of 500 µl of 2 mg/ml OVA in water. Hepes 500 µl (BF) (closed squares) and Hepes 500 µl (AF) (closed circles) correspond to an inner phase of 500 µl of 2 mg/ml OVA in 25 mM Hepes pH 7.4, before and after stirred-cell filtration, respectively. Data presented correspond to 1 batch.

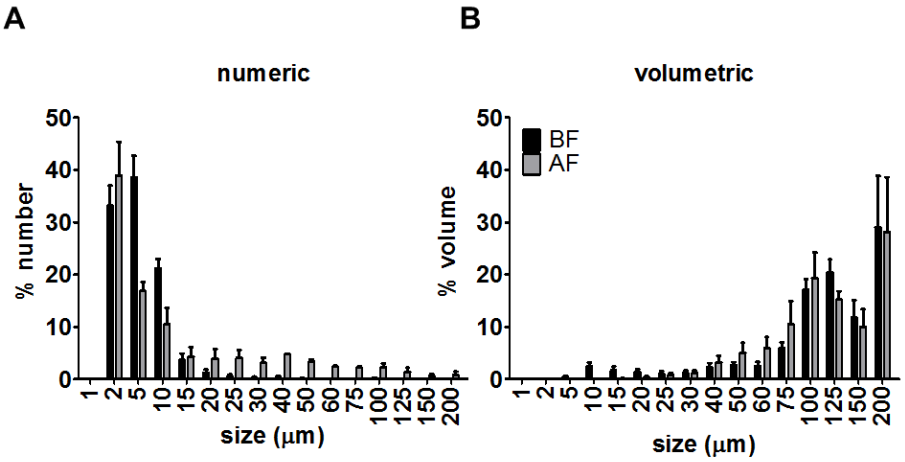

Supplemental Figure 3: Size distribution of MP before filtration (BF) and after filtration (AF) determined by light obscuration. **A)** Number distribution. **B)** Volume distribution. Data are presented as average ± standard deviation of n=3 independent batches.

A) NP 50:50

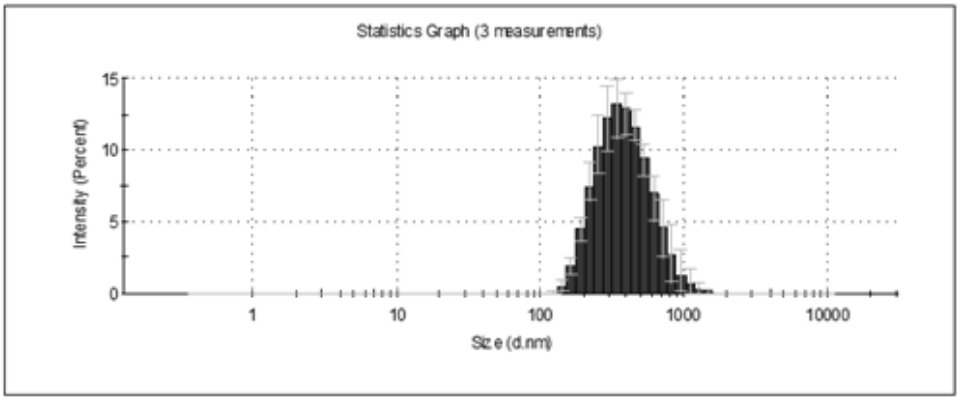

B) NP 75:25

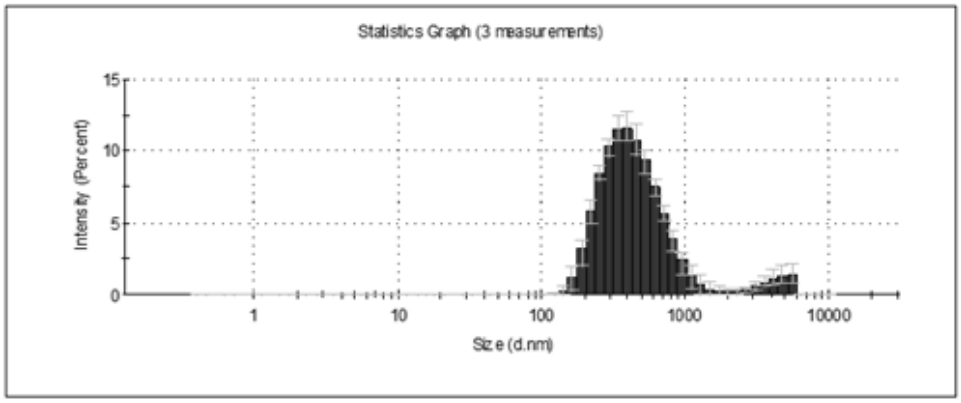

Supplemental Figure 4: Intensity-weighted size distribution of NP determined by DLS. **A)** NP 50:50. **B)** NP 75:25. Data are presented as average ± standard deviation of n=3 independent batches.

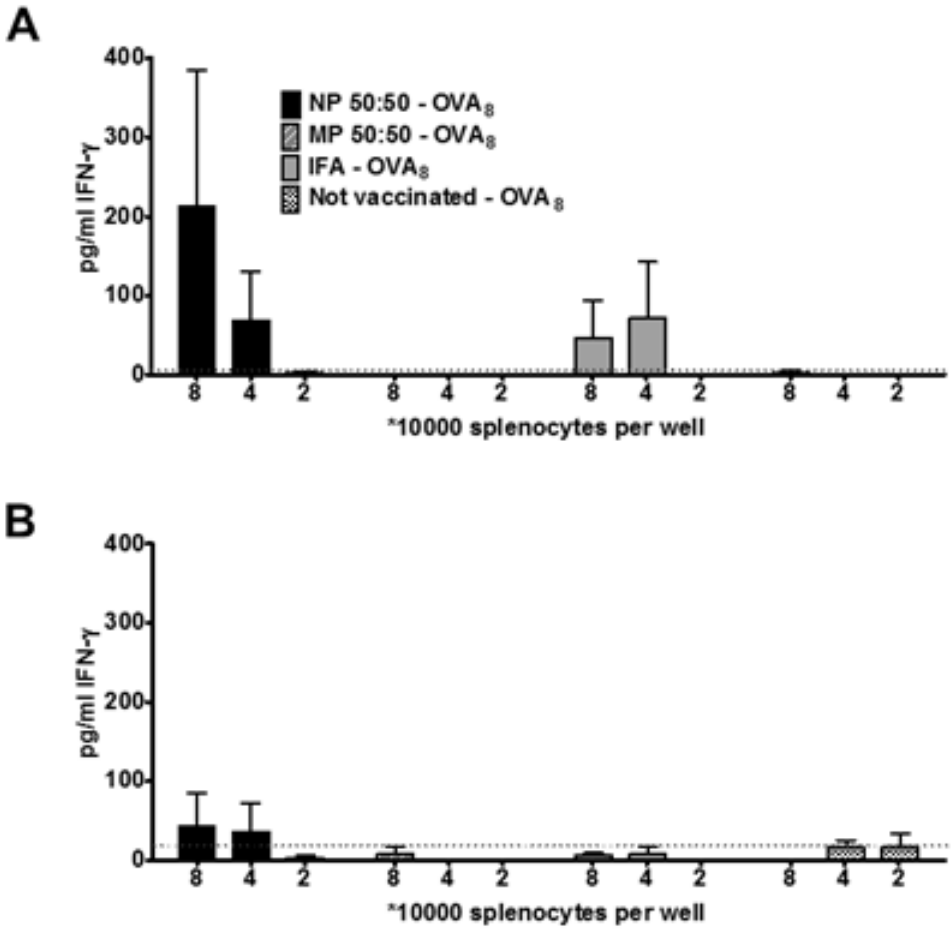

Supplemental Figure 5: IFN-γ production after vaccination with NP. Animals were vaccinated with 50 µg OVA and 20 µg poly(I:C) formulated in NP 50:50, MP 50:50 or in IFA. A) Mice were sacrificed on day 7 post-vaccination, spleens harvested and single cell suspensions re-stimulated with 1 µM SIINFEKL (OVA8). 72 h later the amount of Ag-specific IFN-γ produced was determined by ELISA. B) Animals vaccinated twice (day 0 and 28) were sacrificed on day 42 and the ex vivo IFN-γ production analyzed 72 h later. Red dotted lines indicate average background production of cytokines in the absence of specific stimulation.

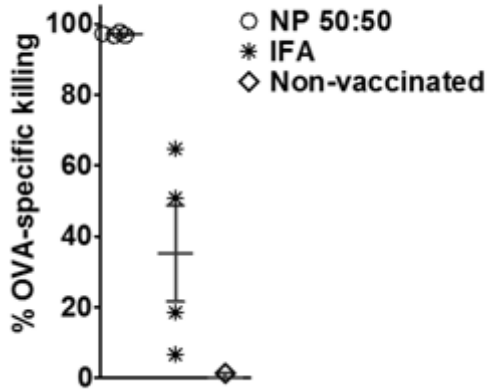

Supplemental Figure 6: PLGA-OVA/poly(I:C) NP induce cytotoxic $CD8^+$ T cells *in vivo*. *In vivo* cytotoxic capacity of primed OVA-specific T cells were determined in animals which received a single s.c. vaccinations with the 50 µg OVA and 20 µg poly(I:C) formulated in NP 50:50 (open circles) or IFA (asterisks), and in non-vaccinated mice (open diamonds). Vaccinated mice received CFSE-labeled OVA8 (specific) or FLU9 (control) short peptide loaded target cells (Ly5.1. splenocytes) 7 days after vaccination. Animals were sacrificed 18 hr later and the % target cells determined flow cytometry and calculated as described in M&M. Results shown are from one experiment and present averages ± SEM from n = 4 mice per group.